**THE EUROPEAN
PHYSICAL JOURNAL B**

Regular Article

Electronic structure of half-metallic ferromagnet Co$_2$MnSi at high-pressure

G. Gökoğlu[1,a] and O. Gülseren[2]

[1] Department of Physics, Karabük University, 78050 Karabük, Turkey
[2] Department of Physics, Bilkent University, 06800 Bilkent, Ankara, Turkey

Abstract. In this study, first principles calculation results of the half-metallic ferromagnetic Heusler compound Co$_2$MnSi are presented. All calculations are based on the spin-polarized generalized gradient approximation (σ-GGA) of the density functional theory and ultrasoft pseudopotentials with plane wave basis. Electronic structure of related compound in cubic $L2_1$ structure is investigated up to 95 GPa uniform hydrostatic pressure. The half-metal to metal transition was observed around $\sim$70 GPa together with downward shift of the conduction band minimum (CBM) and a linear increase of direct band gap of minority spins at Γ-point with increasing pressure. The electronic density of states of minority spins at Fermi level, which are mainly due to the cobalt atoms, become remarkable with increasing pressure resulting a sharp decrease in spin polarization ratio. It can be stated that the pressure affects minority spin states rather than that of majority spins and lead to a slight reconstruction of minority spin states which lie below the Fermi level. In particular, energy band gap of minority spin states in equilibrium structure is obviously not destroyed, but the Fermi level is shifted outside the gap.

1 Introduction

Half-metallic ferromagnetism was first introduced by de Groot et al. [1] in half-Heusler compound NiMnSb which crystallizes in $C1_b$ crystallographic phase. Half-metallic compounds are characterized by metallic electronic band structure for majority spins, while the band structure of minority spins is semiconductor indicating a high spin polarization around Fermi level ($E_{\rm F}$). Consequently, half-metals can conduct a fully spin-polarized current in principal resulting a very large magneto-resistance. 100% spin polarization is a hypothetical situation that can be approached in the limit of vanishing temperature and by neglecting spin-orbit effects [2]. These materials play an important role in various spin-dependent electronic applications like spintronics [3,4], giant magneto-resistance spin valve [5] and spin injection to semiconductors [6–8].

There are several compounds which are predicted to be half-metallic by ab initio calculations [9–13]. The electronic, magnetic and band gap properties of half- and full-Heusler compounds were studied extensively in previous works [14,15]. The electronic and spin-polarization properties of half-metallic Heusler alloys were also reviewed in a recent ab initio study [16]. Co-based full-Heusler compounds (Co$_2$YZ) in cubic $L2_1$ structure, specially Co$_2$MnSi, are the most promising materials for spintronics applications due to high Curie temperature

($T_c = 985$ K) [17], wide band gap in minority spins [13] and easy to synthesize experimentally. Co$_2$FeSi is also a very promising material with 1100 K Curie temperature and 6 μ_B magnetic moment [18]. Co-based Heusler compounds were investigated theoretically in view of density functional calculations and most of them are predicted to be half-metallic [11–14,17,19,20]. Specially, Co$_2$MnSi compound was used in production of thin films [21–23] and devices [24,25] by several groups.

The Heusler alloys are considered to be an ideal local moment system [26,27] and the origin of the half-metalicity of these compounds is more complex than in the half-Heusler alloys due to the presence of the states located entirely at the Co sites [14,28]. Kurtulus et al. studied the magnetic exchange interactions for a series of Heusler compounds including Co$_2$MnZ (Z = Ga, Si, Ge, Sn) by TB-LMTO-ASA method within LDA formalism [29]. They reported that the pair exchange interaction parameter of Co-Mn is much larger than the others in Co$_2$MnSi and Co-Mn interactions are responsible for the stability of ferromagnetism.

The integer magnetic moment is an important characteristic property for these systems in stoichiometric composition. The small deviations from integer magnetic moment lead significant disruptions in half-metallic character by non-zero electronic density of states for minority spins around Fermi level. It is also an important question that in what conditions half-metallic character is

[a] e-mail: ggokoglu@gmail.com

preserved. Some compounds show half-metallic property in bulk structure, but half-metallism is destroyed when surface effects are taken into account [30]. Hashemifar et al. demonstrated that half-metalicity of Co_2MnSi can be preserved by appropriate termination at the (001) surface by ab initio calculations [33]. Ritchie et al. studied the magnetic, structural and transport properties of Co_2MnSi and NiMnSb compounds experimentally [34]. They reported relatively low spin polarizations as: $\sim$45% and $\sim$55% together with non-integer saturation magnetic moments 4.02 and 4.78 μ_B for NiMnSb and Co_2MnSi, respectively. They attribute the obtained results to surface effects (e.g., surface segregation) and antisite disorder. For polycrystalline bulk Co_2MnSi, there is not any Mn-Si type antisite disorder, but Mn-Co type disorders were observed at a level between 10 and 14% as suggested by neutron-diffraction experiments [35]. Since Mn-Co pair exchange interactions are responsible for the stability of ferromagnetic state of Co_2MnSi, Mn-Co disorders can largely change the electronic structure of this compound resulting a disrupted half-metallic behavior.

Until now, high-pressure induced metallization behavior was observed in the non-magnetic insulator and semiconductor compounds and organic molecular crystals rather than half-metallic ferromagnetic structures. One example is barium chalcogenides (BaTe, BaSe, BaS) which are large gap insulators with closed shell ionic system. High pressure optical absorption data on BaS show that the metallization occurs about 80 GPa by band overlap [36]. However, there is not any study in the literature investigating the electronic structure and the stability of half-metallic behavior under high pressure conditions. The major aim of the present work is to clarify the stability of half-metallic electronic structure of cubic Co_2MnSi ($L2_1$) up to 95 GPa pressure in view of the first principles density functional calculations.

2 The Heusler structure and computational method

The full-Heusler alloys are ternary intermetallic compounds based on the X_2YZ stoichiometry for the $L2_1$ phase ($Fm\overline{3}m$ space group, #225). X atoms are transition metals which stand on (0 0 0) and $(\frac{1}{2}\ \frac{1}{2}\ \frac{1}{2})$ Wyckoff crystallographic positions, while Y and Z are magnetic transition metal and III-V group element occupying the positions $(\frac{1}{4}\ \frac{1}{4}\ \frac{1}{4})$ and $(\frac{3}{4}\ \frac{3}{4}\ \frac{3}{4})$, respectively. The importance of these materials arise from the ferromagnetic behavior, even though none of the atoms in the composition is ferromagnetic.

Spin-polarized GGA (Generalized Gradient Approximation) of the Density Functional Theory [37,38] (DFT) was used to approximate exchange correlation potential with Perdew-Burke-Ernzerhof parameterization [39]. It is important the utilization of GGA functionals, which is more successful in description of the physical properties of Heusler compounds than L(S)DA so the obtained results are in better agreement with experiments. Ultrasoft pseudopotentials are generated by scalar relativistic
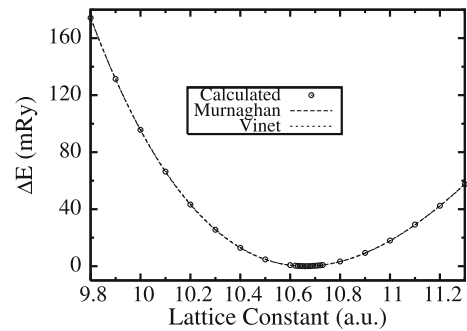

Fig. 1. Energy relative to equilibrium energy as a function of lattice constant and fit curves according to Vinet and Murnaghan equation of states.

calculation for Co and Mn and non-relativistic calculation for Si atoms with non-linear core correction. The valance states of the atoms considered are as follows: Co: $3d^8\ 4s^1$, Mn: $3s^2\ 3p^6\ 4s^2\ 3d^5$, Si: $3s^2\ 3p^2$. Brillouin zone integration was performed with automatically generated $15 \times 15 \times 15$ k-point mesh following the convention of Monkhorst and Pack [40] yielding 240 k points in the irreducible wedge of the Brillouin zone centered at Γ-point. Wave-functions were expanded in plane wave basis sets up to a kinetic energy cut-off value of 1224 eV. This corresponds to about 2680 plane waves. These values are tested and determined to provide convergence in self-consistent calculations. Methfessel-Paxton type smearing was applied on fermionic occupation function with $\sigma = 0.25$ eV smearing parameter [41]. The Kohn-Sham equations were solved by iterative Davidson type diagonalization method [42] with 1×10^{-8} Ry energy convergence threshold. Spin-orbit effects and non-collinear configurations are neglected in calculation procedure.

The static equation of states of the system was constructed using Vinet equation of states [43], which is found to be most accurate among the several equation of states formulations in a previous comprehensive study [44]. The pressure for each volume is calculated analytically from the first derivative of the Vinet equation according to volume. The fits are performed using total energies at 27 different volumes ranging from 0.78 to 1.2 V_0.

3 Results and discussion

The calculated total energy as a function of lattice constant of stoichiometric Co_2MnSi was shown in Figure 1. We fit these data to Vinet [43] and Murnaghan [45] equation of states in order to obtain equilibrium structural parameters of the cubic $L2_1$ system. The root-mean-square errors in energy obtained in the fitting process were 5×10^{-7} and 1×10^{-5} Ry for Vinet and Murnaghan equation of states, respectively. Therefore, we list the Vinet parameters in Table 1 due to very low errors in energy and more accuracy. The bulk modulus calculated from Murnaghan was 210 GPa with the same equilibrium lattice constant value. The calculated lattice constant and total magnetic moment of the system are in very good

Table 1. Calculated, theoretical and experimental values of equilibrium structural parameters of Co_2MnSi.

	a (a.u.)	μ (μ_B)	B (GPa)	B'
Present work	10.66	5.00	214	4.674
Ref. [12] (GGA)	10.65	5.00	226	–
Ref. [12] (LDA)	10.42	5.00	264	–
Exp. [31,32]	10.68	$5.01 \leq \mu \leq 5.15$	–	–
Exp. [47]	10.685	5.07	–	–

agreement with the available experimental data and other ab initio calculations. But the LSDA results of reference [12] based on von Barth-Hedin parameterization underestimate the equilibrium volume by ∼7% with respect to experiment resulting a relatively large bulk modulus value.

Co_2MnSi system obeys the Slater-Pauling rule with integer saturation magnetic moment which scales with the number of valance electrons. According to this rule, total magnetic moment of the system is expressed as: $M_t = Z_t - 24$ for full-Heusler compounds, where Z_t is the number of valance electrons ($Z_t = 29$ for Co_2MnSi). This situation also results 100 % spin polarization at Fermi level. The non-integer magnetic moments observed in experiments lead to low spin-polarization ratios at Fermi level [34]. Note that the spin polarization and magnetic moment of the system is very sensitive to calculation conditions. The relatively small changes in lattice constants and slight deviations from equilibrium state result remarkable changes of magnetic moment values in collinear spin-polarized calculations. In Table 2, we have shown the calculated total and partial magnetic moments of Co_2MnSi. The magnetic moment of the system is largely localized on Mn site with a value of ∼3.3 μ_B. The decrease of magnetic moment of Mn atom is remarkable with increasing pressure. This decrease is mainly due to the Mn d-states in which spin up states are decreased, while spin down states are increased with increasing pressure yielding a lower polarization. The decrease of Mn magnetic moment is compensated to a large extent by the increased magnetic moment of Co site and large suppression of negative contribution of Si atom. The difference in total and absolute magnetizations of the system can also provide information about the spin configurations in the crystal structure. In our case, this difference $\triangle\mu = |\mu_{tot} - \mu_{abs}|$ changes from 0.43 μ_B at zero pressure to 0.18 μ_B at 95 GPa. This situation is also related to the decreasing negative magnetic moment of Si atom with pressure.

The effect of pressure induces interesting physical properties in some crystal structures. There are several binary compounds which are known to show structural phase transitions under pressure. In some cases, these structural transitions occur with dramatic changes in electronic band structures. An interesting example is half-metallic ferromagnet GdN, whose ground state electronic structure is still an open problem. This compound undergoes a phase transition from rocksalt to zincblende structure for extended lattice parameter (i.e., negative pressure) and from half-metallic rocksalt ($B1$) to a semiconducting hexagonal wurtzite ($B4$) structure
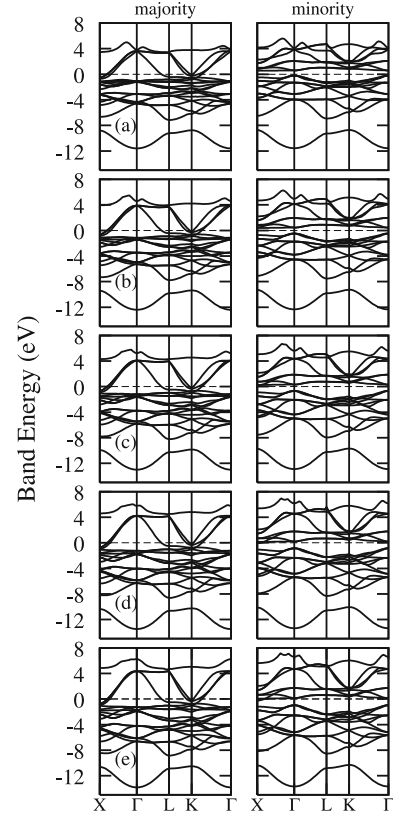
Fig. 2. Spin resolved electronic band structure of Co_2MnSi for majority ($\uparrow$) and minority ($\downarrow$) spins under (a): 0, (b): 25, (c): 50, (d): 75, and (e): 95 GPa pressures.

Table 2. Calculated values of total and partial magnetic moments (in μ_B) of Co_2MnSi at various pressures.

P (GPa)	Total	Co	Mn	Si
0	5.00	0.93	3.30	–0.12
25	5.01	0.96	3.21	–0.08
50	5.03	0.98	3.15	–0.05
75	5.02	0.98	3.11	–0.03
95	4.98	0.98	3.06	–0.02

under hydrostatic pressure [46]. But our GGA calculations of Co_2MnSi system present rather interesting behavior, in which the $L2_1$ crystallographic phase remains stable, when system undergoes a half-metal to metal transition with increasing pressure.

In Figure 2, we show the GGA calculated spin-polarized electronic band structures of Co_2MnSi under 0, 25, 50, 75, and 95 GPa uniform hydrostatic pressures.
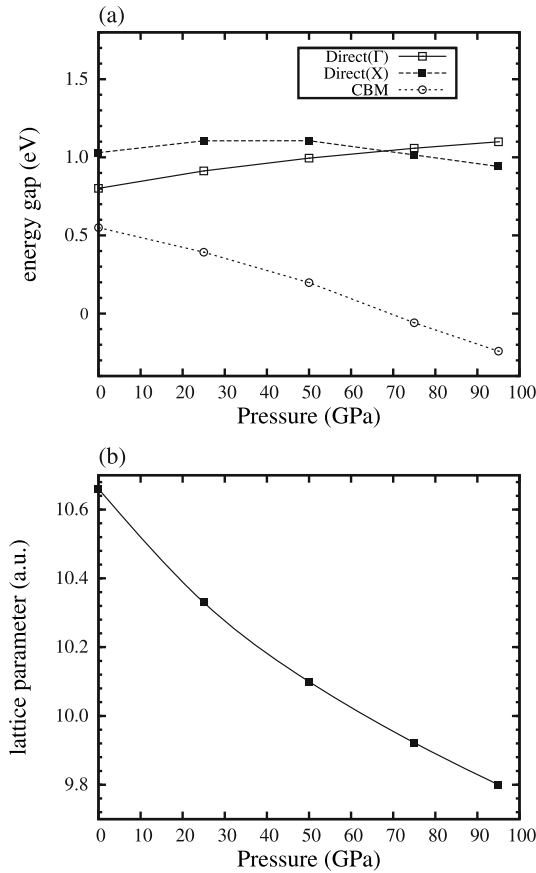
Fig. 3. Minority spin energy band gap values (a) and lattice parameter (b) as a function of pressure.

Fig. 4. Spin resolved electronic density of states of Co_2MnSi projected on Co (solid line), Mn (long dashed line), and Si (short dashed line) atoms for (a): 0, (b): 25, (c): 50, (d): 75, and (e): 95 GPa pressures.

The equilibrium electronic bands of the compound is half-metallic with strongly metallic behavior for majority ($\uparrow$) and semiconducting behavior for minority ($\downarrow$) spin states. The zero pressure band structures are in excellent agreement with the previously reported full-potential linearized augmented plane wave (FLAPW) calculations [12]. The indirect energy band gap along Γ-X in minority spins is 0.76 eV and was calculated as 0.81 eV in reference [12]. The lowest energy bands for both up and down spin states between –12 and –8 eV are mainly due to Si electrons without any hybridization. It is interesting that there is an upward shift at highest energy conduction bands and a downward shift at lowest energy valance bands with increasing pressure for both up and down states. Moreover, the amount of shifts are approximately same ($\sim$1.5 eV) in the studied pressure range. The degeneracy of the Γ-point majority spin bands around ~-1.1 eV at zero pressure is removed with increasing pressure and these bands become well separated at 95 GPa. The same situation was not encountered at minority states and all degeneracies at Γ-point are preserved without any splitting. There is a remarkable downward shift (relative to Fermi level) at the bands around Fermi level for both majority and minority spins with increasing pressure. In Figure 3, we show the energy band gap values as a function of pressure for minority spin
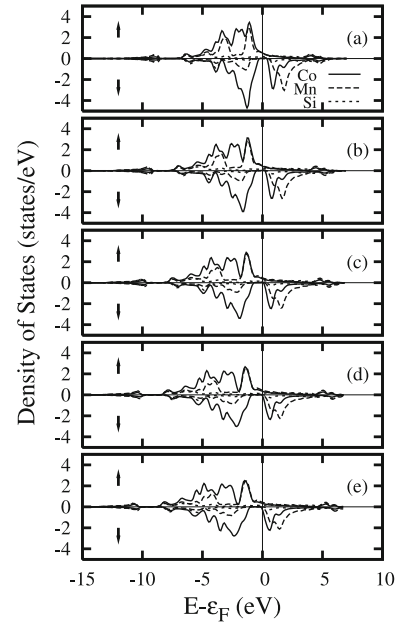
states, which is responsible for pressure induced metalization of the system. The third line in the figure labelled as CBM (conduction band minimum) measures the distance of the lowest energy conduction band to the Fermi level at X-point. The direct band gap at Γ-point changes almost linearly with pressure. In this case, the change of CBM with pressure can be used to determine the half-metal to metal transition pressure, because there is only one band at X-point crossing the Fermi level with increasing pressure. The transition pressure was determined as 70 GPa at which CBM touches the Fermi level. This pressure value corresponds to the contraction of the lattice by a volume ratio of $V/V_0 = 0.81$. The important point which should be mentioned that the overall shape of the band structure for both majority and minority spin states do not change with increasing pressure as an indication of the robustness of electronic structure of Co_2MnSi system. This property has also an important impact on thin films where the lattice parameter can be changed slightly by the growth on a substrate with lattice mismatch. This feature makes the Co_2MnSi a successful material specially in tuneling magnetoresistive (TMR) devices. The critical enlarged upper lattice parameter of the system falls out of the studied range ($a = 9.8$ a.u. $\Rightarrow$ 11.2 a.u.). The extended lattices with lattice parameters $a = 10.66$ a.u. $\Rightarrow$ 11.2 a.u. preserve half-metallic character.

The effects of pressure can be better understood with the electronic density of states at related pressures. Spin resolved partial electronic density of states of Co_2MnSi was shown in Figure 4. The main contributions to electronic density of states come from the 3d-states of Co and Mn atoms, while the contributions of s- and p-states are approximately ten times smaller than 3d states. The
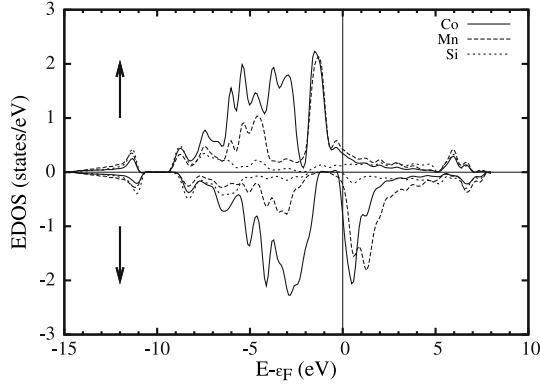
Fig. 5. Spin resolved site projected electronic density of states of Co_2MnSi at $P = 150$ GPa.

densities of s- and p-states of Si atom are very close to each other and are much smaller than that of other atoms. Hence the electronic bands around the Fermi level are largely due to the hybridization of Co and Mn $3d$-states. There are 8 Co atoms surrounding the Mn atom in $L2_1$ structure, this also increases the hybridization of $3d$-states of Co and Mn atoms.

It is clearly seen from the figure that the majority spin densities at Fermi level are mainly caused by the cobalt atoms. Fermi level shifts from 15.4063 eV at zero pressure to 21.0999 eV at 95 GPa. The non-zero minority spin densities at high pressures are also due to the cobalt atoms. The spin polarization ratio at Fermi level, which is defined as $(D_\uparrow - D_\downarrow)/(D_\uparrow + D_\downarrow)$, decreases to 0.97 and to 0.34 at 75 and 95 GPa, respectively. Note that the polarization value at 95 GPa is comparable to that of ordinary metallic ferromagnets. The most dramatic effect of pressure is seen at minority spin states of cobalt atoms below the Fermi level. The strong peak of Co ($\downarrow$) states around $\sim$−1.3 eV at zero pressure shifts to $\sim$−2.4 eV at $P = 95$ GPa together with a remarkable decrease in states density from $\sim$−5 states/eV to $\sim$−2.8 states/eV. The minority states of Mn atom are mainly located above the Fermi level at $\sim$1.8 eV energy of zero pressure. The states located above the Fermi level, which are mostly minority states, show relatively small shifts ($\sim$0.4 eV) in comparison to states below the Fermi level with increasing pressure.

The robustness of the electronic structure is seen in electronic density of states as well as in band structures. In order to see the behavior at extremely high pressures, we have also calculated partial electronic density of states at $P = 150$ GPa as shown in Figure 5. As seen from this figure, the overall shape of the electronic states do not change except from an increase in Fermi level. Although this pressure value is extremely high, the obtained picture shows that the electronic structure of the system does not collapse indicating a very stable electronic phase.

4 Conclusion

The electronic properties of Co_2MnSi half-metallic Heusler system were studied by ab initio density functional calculations even at equilibrium and elevated pressures. GGA calculated structural parameters are in excellent agreement with experiments. The metallization occurs at 70 GPa with monotonic decrease of conduction band minimum upon increasing pressure. The volume of the original lattice is contracted by a volume ratio of 0.81 at this pressure value. The electronic structure of the system are largely determined by the hybridization of the d-electronic states of Co and Mn atoms. The perfect half-metallism of the system at equilibrium (i.e. zero pressure) is destroyed at elevated pressures yielding $R = 0.34$ spin polarization ratio at 95 GPa. The general characteristics of energy band structure is maintained with increasing pressure, but the Fermi level is shifted to higher energy. This situation can be attributed to rigid electronic structure of the system under study.

References

1. R.A. de Groot, F.M. Mueller, P.G. Van Engen, K.H.J. Buschow, Phys. Rev. Lett. **50**, 2024 (1983)
2. M.I. Katsnelson, V.Yu. Irkhin, L. Chioncel, A.I. Lichtenstein, R.A. de Groot, Rev. Mod. Phys. **80**, 315 (2008)
3. V.Yu. Irkhin, M.I. Katsnelson, Usp. Fiz. Nauk **164**, 705 (1994), [Phys. Usp. **37**, 659 (1994)]
4. I. Zutič, J. Fabian, S. Das Sarma, Rev. Mod. Phys. **76**, 323 (2004)
5. B. Dieny, V.S. Speriosu, S.S.P. Parkin, B.A. Gurney, D.R. Wilhoit, D. Mauri, Phys. Rev. B **43**, 1297 (1991)
6. G. Schmidt, D. Ferrand, L.W. Molenkamp, A.T. Filip, B.J. Van Wees, Phys. Rev. B **62**, R4790 (2000)
7. R. Fiederling, M. Keim, G. Reuscher, W. Ossau, G. Schmidt, A. Waag, L.W. Molenkamp, Nature (London) **402**, 78 (1999)
8. Y. Ohno, D.K. Young, B. Beschhoten, F. Matsukura, H. Ohno, D.D. Awschalom, Nature (London) **402**, 790 (1999)
9. Y. Miura, M. Shirai, K. Nagao, J. Appl. Phys. **99**, 08J112 (2006)
10. H.C. Kandpal, G.H. Fecher, C. Felser, G. Schönhense, Phys. Rev. B **73**, 094422 (2006)
11. M. Shirai, J. Appl. Phys. **93**, 6844 (2003)
12. S. Picozzi, A. Continenza, A.J. Freeman, Phys. Rev. B **66**, 094421 (2002)
13. S. Ishida, S. Fujii, S. Kashiwagi, S. Asano, J. Phys. Soc. Jpn **64**, 2152 (1995)
14. I. Galanakis, P.H. Dederichs, N. Papanikolau, Phys. Rev. B **66**, 174429 (2002)
15. I. Galanakis, P.H. Dederichs, N. Papanikolau, Phys. Rev. B **66**, 134428 (2002)
16. I. Galanakis, Ph. Mavopoulos, J. Phys.: Condens. Matter **19**, 315213 (2007)
17. P.J. Brown, K.U. Neumann, P.J. Webster, K.R.A. Ziebeck, J. Phys.: Condens. Matter **12**, 1827 (2000)

18. S. Wurmehl, G.H. Fecher, H.C. Kandpal, V. Ksenofontov, C. Felser, H.J. Lin, J. Morais, Phys. Rev. B **72**, 184434 (2005)
19. H.C. Kandpal, G.H. Fecher, C. Felser, J. Phys. D: Appl. Phys. **40**, 1507 (2007)
20. T. Block, C. Felser, G. Jakob, J. Ensling, B. Muhling, P. Gutlich, V. Beaumont, F. Studer, R.J. Cava, J. Solid State Chem. **176**, 646 (2003)
21. W.H. Wang, M. Przybylski, W. Kuch, L.I. Chelaru, J. Wang, Y.F. Lu, J. Barthel, J. Kirschner, J. Magn. Magn. Mater. **286**, 336 (2005)
22. W.H. Wang, M. Przybylski, W. Kuch, L.I. Chelaru, J. Wang, Y.F. Lu, J. Barthel, H.L. Meyerheim, J. Kirschner, Phys. Rev. B **71**, 144416 (2005)
23. S. Kaemmerer, S. Heitmann, D. Meyners, D. Sudfeld, A. Thomas, A. Hütten, G. Reiss, J. Appl. Phys. **93**, 7945 (2003)
24. K. Inomata, S. Okamura, N. Tezuka, J. Magn. Magn. Mater. **282**, 269 (2004)
25. S. Kaemmerer, A. Thomas, A. Hütten, G. Reiss, Appl. Phys. Lett. **85**, 79 (2004)
26. A. Hamzič, R. Asomoza, I.A. Campbell, J. Phys. F: Met. Phys. **11**, 1441 (1981)
27. J. Kübler, A.R. Williams, C.B. Sommers, Phys. Rev. B **28**, 1745 (1983)
28. E. Şaşıoğlu, L.M. Sandratskii, P. Bruno, I. Galanakis, Phys. Rev. B **72**, 184415 (2005)
29. Y. Kurtulus, R. Dronskowski, G.D. Samolyuk, V.P. Antropov, Phys. Rev. B **71**, 014425 (2005)
30. G. Lee, I.G. Kim, J.I. Lee, Y.-R. Yang, Phys. Stat. Sol. B **241**, 1435 (2004)
31. P.J. Webster, J. Phys. Chem. Solids **32**, 1221 (1971)
32. M.P. Raphael, S.F. Cheng, B.N. Das, B. Ravel, B. Nadgorny, G. Trotter, E.E. Carpenter, V.G. Harris, MRS Proceedings, Spring Meeting (2001)
33. S.J. Hashemifar, P. Kratzer, M. Scheffler, Phys. Rev. Lett. **94**, 096402 (2005)
34. L. Ritchie, G. Xiao, Y. Ji, T.Y. Chen, C.L. Chien, M. Zhang, J. Chen, Z. Liu, G. Wu, X.X. Zhang, Phys. Rev. B **68**, 104430 (2003)
35. M.P. Raphael, B. Ravel, M.A. Willard, S.F. Cheng, B.N. Das, R.M. Stroud, K.M. Bussmann, J.H. Claassen, V.G. Harris, Appl. Phys. Lett. **79**, 4396 (2001)
36. S.T. Weir, Y.K. Vohra, A.L. Ruoff, Phys. Rev. B **35**, 874 (1987)
37. W. Kohn, L.J. Sham, Phys. Rev. **140**, A1133 (1965)
38. P. Hohenberg, W. Kohn, Phys. Rev. **136**, B864 (1964)
39. J.P. Perdew, K. Burke, M. Ernzerhof, Phys. Rev. Lett. **77**, 3865 (1996)
40. H.J. Monkhorst, J.D. Pack, Phys. Rev. B **13**, 5188 (1976)
41. M. Methfessel, A.T. Paxton, Phys. Rev. B **40**, 3616 (1989)
42. E.R. Davidson, J. Comput. Phys. **17**, 87 (1975)
43. P. Vinet, J. Ferrante, J.R. Smith, J.H. Rose, J. Phys. C **19**, L467 (1986)
44. R.E. Cohen, O. Gülseren, R.J. Hemley, American Mineralogist **85**, 338 (2000)
45. F.D. Murnaghan, Proc. Natl. Acad. Sci. USA **3**, 244 (1944)
46. S. Abdelouahed, M. Alouani, Phys. Rev. B **76**, 214409 (2007)
47. P.J. Webster, K.R.A. Ziebeck, in *Alloys and Compounds of d-elements with Main Group Elements, Part 2*, edited by H.R.J. Wijn, Landolt-Börnstein, New Series, Group III (Springer, Berlin, 1998), Vol. 19/c, pp. 75–184